Heliyon 9 (2023) e15602

Contents lists available at ScienceDirect

Heliyon

journal homepage: www.cell.com/heliyon

Research article

Integrated serum pharmacochemistry and metabolomics reveal potential effective components and mechanisms of Shengjiang Xiexin decoction in the treatment of *Clostridium difficile* infection

Yutao Cui [a,b,c,1], Congen Zhang [a,1], Xueqiang Zhang [a], Xiaohong Yu [a], Yuqin Ma [a], Xuemei Qin [b,**], Zhijie Ma [a,*]

[a] *Beijing Friendship Hospital, Capital Medical University, Beijing, China*
[b] *Modern Research Center for Traditional Chinese Medicine, Shanxi University, Taiyuan, China*
[c] *Bayannur City Hospital, Bayannaoer, China*

ARTICLE INFO

Keywords:
Shengjiang Xiexin Decoction
Clostridium difficile infection
Serum medicinal chemistry
Metabolomes
Pharmacological effects
Bioactive compounds

ABSTRACT

Shengjiang Xiexin Decoction (SXD) is a widely recognized formula in Traditional Chinese Medicine (TCM) for treating diarrhea and is commonly used in clinical practice. *Clostridium difficile* infection (CDI) is a type of antibiotic-associated diarrhea with a rising incidence rate that has severe consequences for humans. Recent clinical applications have found significant efficacy in using SXD as an adjunct to CDI treatment. However, the pharmacodynamic substance basis and therapeutic mechanism of SXD remain unclear. This study aimed to systematically analyze the metabolic mechanisms and key pharmacodynamic components of SXD in CDI mice by combining non-targeted metabolomics of Chinese medicine and serum medicinal chemistry. We established a CDI mouse model to observe the therapeutic effect of SXD on CDI. We investigated the mechanism of action and active substance composition of SXD against CDI by analyzing 16S rDNA gut microbiota, untargeted serum metabolomics, and serum pharmacochemistry. We also constructed a multi-scale, multifactorial network for overall visualization and analysis. Our results showed that SXD significantly reduced fecal toxin levels and attenuated colonic injury in CDI model mice. Additionally, SXD partially restored CDI-induced gut microbiota composition. Non-targeted serum metabolomics studies showed that SXD not only regulated Taurine and hypotaurine metabolism but also metabolic energy and amino acid pathways such as Ascorbate and aldarate metabolism, Glycerolipid metabolism, Pentose and glucuronate interconversions, as well as body and other metabolite production in the host. Through the implementation of network analysis methodologies, we have discerned that Panaxadiol, Methoxylutcolin, Ginsenoside-Rf, Suffruticoside A, and 10 other components serve as critical potential pharmacodynamic substance bases of SXD for CDI. This study reveals the metabolic mechanism and active substance components of SXD for the treatment of CDI mice using phenotypic information, gut microbiome, herbal metabolomics, and serum pharmacochemistry. It provides a theoretical basis for SXD quality control studies.

* Corresponding author. Beijing Friendship Hospital, Capital Medical University, No. 95, Yongan Road, 100050, Beijing, China.
** Corresponding author.
E-mail addresses: qinxm@sxu.edu.cn (X. Qin), mazj2021@163.com (Z. Ma).
[1] These authors contributed equally to this work.

https://doi.org/10.1016/j.heliyon.2023.e15602
Received 22 February 2023; Received in revised form 13 April 2023; Accepted 18 April 2023
Available online 20 April 2023

1. Introduction

A spore-forming gram-positive anaerobic bacillus, *Clostridium difficile* (*C. difficile*), can cause diarrhea and other infections [1]. *C. difficile* infections (CDI) typically occur following the use of antibiotics, which disrupts the normal gut microbiota and allows it to flourish. CDI is one of the major causes of hospital-acquired antibiotic-associated diarrhea in both developing and developed countries [2,3]. *C. difficile* induces intestinal inflammation and diarrhea through the release of Toxin A and Toxin B. Toxin B, which is 10 times more virulent than Toxin A, is the main causative agent of CDI [4–6]. *C. difficile*-associated diarrhea is associated with an inflammatory cascade that affects various mechanisms [7]. Metronidazole and vancomycin are the most common antibiotics used to treat primary *C. difficile* infection, but antibiotic treatment has a high relapse rate [8]. Thus, there is a critical need to develop new therapeutic strategies for CDI.

Shengjiang Xiexin Decoction (SXD), a Chinese medicine prescribed in Shang Han Lun, is a popular treatment for diarrhea, gastroenteritis, and Inflammatory bowel disease. It has also been found to effectively relieve diarrhea caused by antineoplastic drugs [9–11], Importantly, no side effects have been reported in clinical presentations [12]. However, despite its traditional efficacy, research on SXD has been primarily focused on verification, and the mechanism of action and main active ingredients have not been studied in depth. This lack of investigation has limited its clinical application.

The ambiguity of TCM evidence groups and the complexity of TCM prescriptions severely limit the evaluation of prescription effectiveness and identification of the material basis of pharmacological effects. To fully comprehend disease and drug mechanisms at a systems level, it is essential to integrate multidimensional data [13,14]. In such integrated approaches, gut microbiota and metabolite information are crucial to understanding the interactions between the gut microbiota and the host [15]. Therefore, combining metabolomics with herbal serum pharmacochemistry is a promising strategy. It can establish a scientific language to explain the effectiveness of TCM, explore the overall changes in organism metabolites, and identify active ingredients of medicines [16,17].

We hypothesize that SXD's ameliorative effect on CDI is related to its modulation of gut microbiota composition and metabolism. In this study, we first investigated the effect of SXD on CDI mice. Next, we used 16s rDNA gene sequencing, non-targeted metabolomics, and serum pharmacochemistry to detect changes in intestinal flora, metabolism, and blood prototype drug profiles in the mice. Finally, we constructed a multiscale, multifactorial visualization network to characterize the mechanism of action and active ingredients of SXD.

2. Methods

2.1. Experimental animals

At the time of purchase, Spelford Biotechnology Ltd provided a license number for the SPF grade C57BL/6J mice. The mice were kept in a clean-grade laboratory animal room with temperatures maintained between 20 and 22° Celsius, and a 12-h light and dark cycle. Only male mice aged 5–6 weeks were used in this study. The mice were housed in cages with sterile water and food, and all were kept in filtered cages.

2.2. Ethical policies

All animal experiments were conducted in accordance with the NIH Guidelines for Care and Use of Laboratory Animals in the United States and the Prevention of Cruelty to Animals Act of 1986 in China. Additionally, the Animal Ethics Committee of Beijing Friendship Hospital approved the experiments (approval number 22–2018).

Table 1
Information on experimental herbs.

Decoction pieces[a]	Botanical origin	Medicinal parts	Manufacturers	Batch No.	Dose[b]
Zngiberis Rhizoma Recens	*Zingiber officinale* Rosc.	Rizoma (Fresh)	Beijing Renwei Chinese Medicine Tablet Factory	20110404	12 g
Zingiberis Rhizoma	*Zingiber officinale* Rosc.	Rizoma (Dried)	Beijing Qiancao Beverage Tablets Co.	20093003	3 g
Ginseng Radix Et Rhizoma	*Panax ginseng* C. A. Mey.	Radix et Rhizoma	Beijing Tongchuntang Pharmaceutic al Co.	1906005	9 g
Pinelliae Rhizoma Praeparatum	*Pinellia ternata* Breit.	Rizoma	Beijing Tongrentang Beverage Tablets Co.	1231144	9 g
Glycyrrhizae Radix et RhizomaPraeparata Cum Melle	*Glycyrrhiza uralensis* Fisch.	Radix et Rhizoma	Beijing Yanbei Beverage Tablets Factory	200516	9 g
Scutellariae Radix	*Scutellaria baicalensis* Georgi.	Radix	Beijing Shuangqiao Yanjing Chinese Medicine Tablet Factory	1912204	9 g
Coptidis Rhizoma	*Coptis chinensis* Franch.	Rhizoma	Beijing Shuangqiao Yanjing Chinese Medicine Tablet Factory	1912205	3 g
Jujubae Fructus	*Ziziphus jujuba* Mill.	Fructus	Beijing Qiancao Beverage Tablets Co.	201105005	9 g

[a] The traditional Chinese medicine decoction pieces included in SXD are in accordance with Chinese Pharmacopoeia.
[b] According to the "Treatise on Febrile Diseases (*Shang Han Lun*)," decoction pieces in SXD should be taken daily.

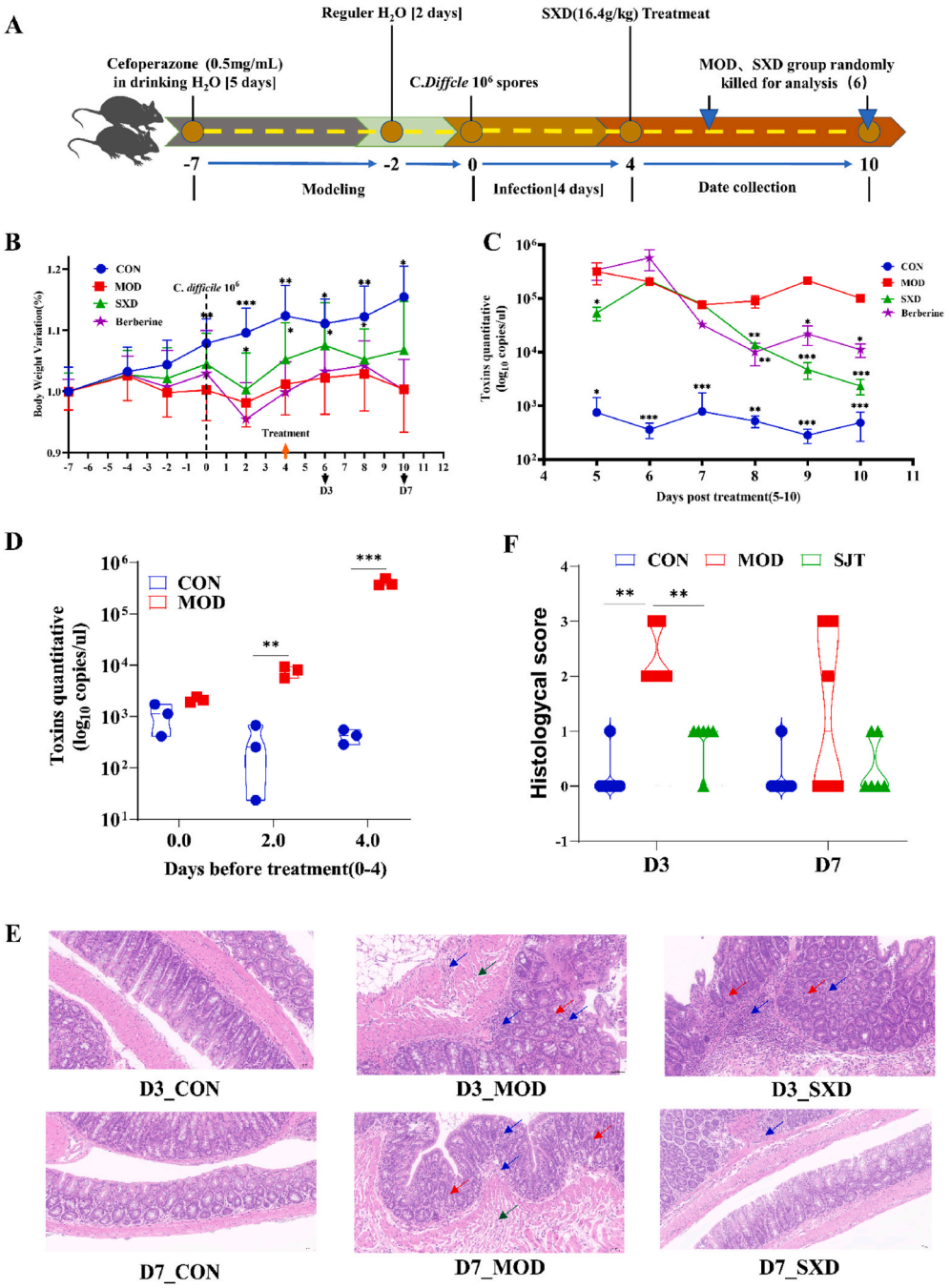

Fig. 1. Ameliorative effect of SXD on *C. difficile*-induced colitis. (A) Cefoperazone replacement of drinking water for 5 days during the model construction period (days −7 to −1), followed by replacement of normal drinking water for mice infected with *C. difficile* (days 0 to 3), and SXD 16.4 g.kg-1 during the treatment period (days 4 to 10). (B) Body weight variation of mice in each group throughout the experiment (n = 6). (C–D) Quantification of fecal toxin levels in mice infected with *C. difficile* (n = 3). (E) Representative histopathological sections showing small focal necrosis of colonic tissue (black arrows), inflammatory cell infiltration (blue arrows); crypt nuclear division phenomenon (red arrows), scale bar, 50 μm (n = 6). (F) Histological score of mice ± treatment with SXD (n = 5). Data are expressed as mean ± SEM and ANOVA with post hoc test was used to calculate significant differences, $*P < 0.05$, $**P < 0.01$, $***P < 0.001$. (For interpretation of the references to colour in this figure legend, the reader is referred to the Web version of this article.)

2.3. C. difficile strains

C. difficile 630 (ATCC BAA-1382) was obtained from the Laboratory Department of Beijing Friendship Hospital and inoculated onto Columbia blood plates in a standard anaerobic environment. The plates were then incubated at a constant temperature of 37 °C for 7 days to allow the colonies to produce a large number of *C. difficile* spores. Using a sterile loop, colonies were removed from the Petri dishes and resuspended in sterile phosphate-buffered saline (PBS).

To isolate only the spores, the cell suspension was heated in a water bath at 65 °C for 20 min to kill the *C. difficile* trophic cells. After heating, the suspension was centrifuged at 3000×*g* using blow centrifugation with 2–3 washes, and the resulting precipitate was resuspended in a cryopreservation solution. The solution was then stored at −80 °C for later use.

2.4. Herbal and chemical materials

For research, SXD consists of eight herbs: fresh rioma of *Zingiber officinale* Rosc., dried rioma of *Zingiber officinale* Rosc., *Panax ginseng* C. A. Mey., *Pinellia ternata* Breit., *Glycyrrhiza uralensis* Fisch., *Scutellaria baicalensis* Georgi., *Coptis chinensis* Franch., *Ziziphus jujuba* Mill., the information is shown in Table 1. The herbs were authenticated by Professor Zhao Kuijun of Beijing Friendship Hospital, Capital Medical University. Cefoperazone was supplied by Yuanye Bio-Technology Co. Ltd (Y09m8c30304, Shanghai, China). Berberine was supplied by the Chinese National Institutes for Food and Drug Control (110713–201814, Beijing, China).

2.5. SXD solution extract preparation

Conventional methods were used for water extraction. The herbs were soaked in water (1:8, w/v) for 30 min and then heated by refluxing for 60 min. The resulting filtrate was collected, and the residue was refluxed again in water (1:6, w/v) for 60 min. The two filtrates were combined and then concentrated to a volume of 80 ml, which had a raw drug concentration of 0.79 g/ml. The resulting solution was cooled to 4 °C, refrigerated, and reserved.

2.6. Chemical analysis and quality control of SXD

Chromatographic analysis was conducted using a Shimadzu LC-IT-TOF-MS system. Details of the methods and chromatograms are available in the supplementary material (Fig. S1). The contents of 17 key active components, including 6-gingerol, curcumin, baicalein, baicalin, wogonin, berberine chloride, coptisine, epi berberine, palmatine chloride, ginsenoside Rb1, ginsenoside Re, ginsenoside Rg1, glycyrrhizic acid, liquidity, rutin, ursolic acid, and trigonelline, were determined using a Waters UPLC-Xevo-TQS microsystem (Supplementary Table 1). Various target compounds were measured in SXD extracts at different transport rates. Additionally, quantitative analysis of SXD was performed using a Q-Exactive system from Thermo Scientific Technologies (Waltham, MA, USA). The methodology and chromatograms are provided in the supplementary materials (Supplementary Table 2, Fig. S2, and Fig. S3).

2.7. Experimental design

Before the experiment, the mice were kept stable for one week under conventional feeding conditions. C57BL/6 mice were randomly divided into three groups. The CON group was fed with a normal diet and water daily, while the model group and SXD administration group were treated with 0.5 mg/ml of Cefoperazone instead of drinking water for five days (−7 to −2 days) to disrupt the intestinal flora of the mice. This was followed by replacement with normal drinking water for two days (−2 to 0 days). On day 0, each mouse was challenged with 106 CFU of *C. difficile*, and all mice were fed and watered normally for 0–4 days to allow *C. difficile* bacilli to germinate and colonize in the mice. From day 4 until the end of the experiment (day 10), mice in the treatment group were orally administered SXD at a dose of 16.4 g/kg/day, which is equivalent to two times the human equivalent dose. Six mice in the MOD and SXD groups were randomly sacrificed on day 6, respectively. All mice were executed for sampling on day 7 (see Fig. 1 A).

2.8. Absolute quantitative analysis of C. difficile TcdB coding gene

Supplementary Table 3 presents the primer and probe sequences used in this study. For quantitative polymerase chain reaction (qPCR), a 25 μl reaction system was prepared by adding 12.5 μl of Premix Ex Taq TM (RR390, TAKARA), 0.5 μL Rox Reference Dye II (AK60353A, TAKARA), 2.5 μl of forward and reverse primers and TaqMan probes (1927827100, Sangon Biotech), and 2 μl of DNA. Reactions were run in triplicate on a 7500FAST Real-Time Fluorescence Quantitative PCR Instrument (Thermo Fisher Scientific) under the following conditions: The first step consisted of 1 cycle of 95 °C for 30s, step 2 included 3s of 95 °C and 40 cycles of 50 °C for 30s.

DNA was extracted from mouse feces using the E. Z.N.A.® Stool DNA Kit (00D4015010000J11S001, OMEGA). To construct standard curves, the log10 values of spore quantities corresponding to each DNA dilution were plotted against the Ct values.

2.9. Histopathological analysis

After the observation period, the mice were euthanized, and their colon tissue was taken and fixed in 4% (w/v) paraformaldehyde. The tissue was then embedded in paraffin, sectioned at 5 μm, and stained with hematoxylin and eosin (HE). The pathological tissue

images were evaluated in a single-blind manner by Wuhan Servicebio Technology Co., Ltd., using the following grading criteria: ulceration, mitotic activity, mucus depletion, mononuclear infiltrate, granulocyte infiltrate, and edema. The scoring range was between 0 and 3 points when viewed under a fluorescence microscope.

2.10. Fecal 16S DNA sequencing analysis

On the last day of the experiment, the mice in each group were sacrificed, and their feces were collected aseptically from the colonic area of each group. The samples were then transferred to lyophilized tubes, quenched in a tank of liquid nitrogen for 30 min, and stored in a −80 °C refrigerator. Total DNA was extracted from the feces samples, and the concentration and purity of DNA were measured by an ultra-micro spectrophotometer. The quality of DNA extraction was also evaluated using 1% agarose gel electrophoresis.

Polymerase chain reaction (PCR) amplification of the V3–V4 variable region was performed using 338F and 806R primers. The amplification procedure included pre-denaturation at 95 °C for 3 min, followed by 27 cycles of denaturation at 95 °C for 30 s, annealing at 55 °C for 30 s, and extension at 72 °C for 30 s. The amplification system consisted of 20 μl of reaction mixture, which included 4 μl of 5 × FastPfu buffer, 2 μl of 2.5 mM dNTPs, 0.8 μl of primer (5 μM), 0.4 μl of FastPfu polymerase, and 10 ng of DNA template.

Purified amplification products were mixed and paired for sequencing on the Illumina MiSeq platform (Illumina, USA) following standard operating protocols. The analysis was conducted using Qiime2docs' "moving picture tutorial" and "Atacama soil microbiome tutorial" and specific program scripts. The Qiime2 DADA2 plugin was used to generate Amplicon Sequence Variant (ASV) tables, which performed double-ended read splicing, quality filtering, and chimeric variant filtering. The Sklearn classifier algorithm was used to annotate the classification of each ASV representative sequence against the Greengenes database version 13_8 (99% OTU dataset).

2.11. Sample preparation of serum and SXD extract solution for untargeted metabolomics analysis

First, the mixed internal standard (4-chloro-Dr-phenylalanine) master batch was diluted with methanol to a concentration of about 500 ng/ml to obtain the mixed internal standard solution. Then, 80 μl of frozen serum sample was thawed at 4 °C and mixed with 10 μl of the internal standard solution and 300 μl of refrigerated acetonitrile. The mixture was vortexed for 5 min at 2500 rpm, followed by centrifugation at 15000 rpm for 5 min at 4 °C. The supernatant was removed, and the solvent was evaporated by centrifugation. Next, 100 μl of water/acetonitrile (98:2, v/v) was added, and the mixture was vortexed for 5 min at 2500 rpm. The sample was then centrifuged at 15,000 rpm for 5 min at 4 °C, and the supernatant was removed and filtered.

For the frozen SXD extracts, they were thawed at 4 °C, sonicated to dissolve all samples, and diluted to 1 μg/ml in water/acetonitrile (98:2, v/v). The samples were then prepared by centrifugation at 15,000 rpm for 5 min at 4 °C.

2.12. UPLC-MS profiling of serum and SXD extract solution

Metabolites from serum and drug samples were analyzed using ultra-performance liquid chromatography-mass spectrometry (UPLC-MS), under identical chromatographic and mass spectrometric conditions. Chromatographic separation was carried out using ACQUITY HSS T3 (Waters, USA) and ACQUITY UPLC HSS T3 columns (2.1 × 100 mm, 1.8 μm) (Waters, USA). The column temperature was maintained at 35 °C, and metabolites were detected using a mass spectrometer detector Q-Exactive (Thermo Fisher Scientific, USA). For metabolite detection, 5 μl of sample solution was used. The mobile phase consisted of a mixture of solvent A (H2O, containing 0.1% formic acid) and solvent B (CH3CN) with linear gradient elution. The mass spectrometry conditions were set as follows: spray voltage of 3.5/-3.2 kV, 40/45 Sheath gas, 11/10 AUX gas flow, and a capillary temperature of 350 °C. The mass charge ratio (M/Z) scan range was collected from 70 DA to 1000 DA in both positive and negative modes. To ensure system stability and reproducibility, combined QC samples were analyzed every 10 runs when analyzing serum samples.

2.13. Multivariate statistical analysis and data pre-processing

The raw UPLC-MS data in Wiff format were pre-processed using Progenesis QI software version 2.0 (Waters Corp, Milford, MA, USA). This includes peak identification, peak alignment, peak picking, and data normalization. To determine the differences between groups, principal component analysis (PCA) was performed using SIMCA 14.1 software (Umetrics, Sweden). The variable importance projection (VIP) value was calculated by orthogonal partial least squares discriminant analysis (OPLS-DA), which is the statistically normalized abundance of the different ions. In the OPLS-DA model, variables with VIP $\geq$1.0 were kept. Variables exhibiting a dose-effect relationship and considered to be differential metabolites were identified by using one-way analysis of variance (ANOVA) and *t*-test ($p < 0.05$). The differential metabolites were identified by matching exact *m/z* values between online and local databases, such as the METLIN database (https://metlin.scripps.edu/), the HMDB database (https://hmdb.ca/), and the KEGG database (https://www.kegg.jp/).

2.14. Integrated visual network analysis

Multiscale and multifactor networks were constructed to visualize the mechanisms by which SXD handles CDI. Spearman's rank correlations were used to demonstrate the relationships between parameters. Correlation coefficients < -0.6 (OR > 0.6) and $P < 0.05$, generated by IBM SPSS version 26, were retained for network visualization. Subnetworks were merged using Cytoscape version 3.8.1

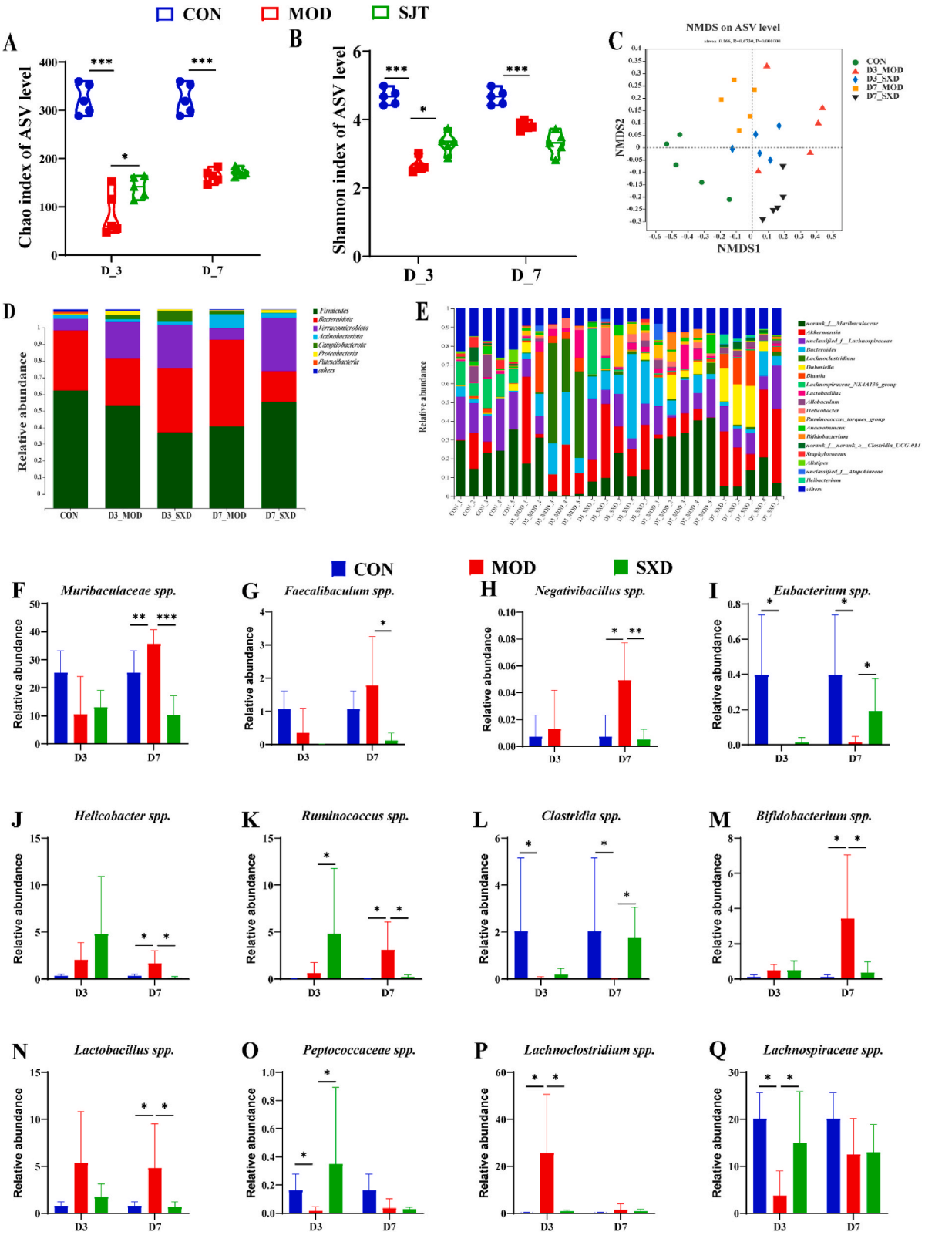

(caption on next page)

Fig. 2. The effects of SXD on gut microbiota. Alpha diversity indicators Chao (A) and Shannon (B) index showing the community diversity and community richness, respectively (n = 4–5). The β-diversity indicators NMDS(C) show the overall variability of the microbiota. (D)Grouping the relative abundance of gut microbiota at the phylum level. (E) Relative abundance of gut microbiota at the genus level. (F–Q) The microbiome disturbed by *C. difficile* recovered after treatment with SXD (n = 4–5). *$P < 0.05$, **$P < 0.01$, ***$P < 0.001$.

to generate the networks.

2.15. Statistical analysis

Statistical significance was determined using the non-parametric Kruskal-Wallis rank sum test, and in cases where this was not applicable, a post hoc analysis of variance (Student-Newman-Keuls test) was conducted. The data are presented as means, and statistical significance was set at $P < 0.05$. The significance levels were denoted as * for $P < 0.05$, ** for $P < 0.01$, and *** for $P < 0.001$. All analysis parameters are listed in Supplementary Table 4.

3. Results

3.1. SXD mitigates C. difficile-induced colitis in mice

Fig. 1B illustrates the body weight changes of mice during the moulding process (days −7 to −2). In the Con group, the body weight increased steadily. In contrast, the Mod, SXD, and Berberine groups showed a decrease in body weight, with a significant difference between the Con and Mod groups at day −2 ($P < 0.05$). During the next phase of the experiment, Gavage *C. difficile* was administered, and mice were left to wait for spore germination (days 0 to 3). During this period, the body weight of mice in the Mod, SXD, and Berberine groups decreased, with the Con and SXD groups displaying higher body weight levels compared to the Mod group ($P < 0.05$). After administration, body weight levels increased gradually in all groups. The SXD group exhibited the most pronounced trend of weight gain, with significant improvements observed on days 2, 4, 6 (D3), and 8 compared to the Mod group ($P < 0.01$ or $P < 0.001$), indicating that SXD improved the symptoms of CDI mice. However, there was no significant difference between the Berberine and MOD groups.

The severity of the disease is closely related to the level of toxins present in the feces [5]. During the modelling period (days 0–4), the fecal toxin levels of mice in the Mod group increased significantly ($P < 0.01$ or $P < 0.001$), indicating successful model replication (Fig. 1D). The toxin levels in the Mod group were evidently higher than those in the Con group during the administration period (days 5–10) ($P < 0.05$, $P < 0.01$, or $P < 0.001$). However, during this period, the toxin levels gradually decreased in the SXD group, and were significantly lower than those in the Mod group on day 5 ($P < 0.05$). By the end of the administration, the toxin level in the SXD group was similar to that of the Con group (Fig. 1C), indicating that SXD could reduce the fecal toxin level in CDI mice. While the Berberine group also showed a reduction in toxin levels compared to the Mod group, the down-regulation of toxin levels by Berberine was weaker than that by SXD, but still significant.

Intestinal tissue injury is a critical feature of CDI [18]. In the Con group, the mucosal epithelium was relatively intact, the crypt of the lamina propria was neatly arranged, the cup cells were abundant, and the submucosal layer and muscular layer were structured. No inflammatory changes were observed. However, in the Mod group, small focal necrosis was occasionally observed in the lamina propria with inflammatory cell infiltration. The columnar cells in the crypt displayed increased nuclear division, and inflammatory cells infiltrated the submucosal layer, indicating that the intestinal tissues had been damaged during the modelling process. On day 3, the intestinal mucosa of the SXD group was intact, with a small amount of inflammatory cell infiltration in the lamina propria. By the end of treatment (day 7), the intestinal tissues of the SXD group had recovered well, with no obvious inflammatory infiltration and only a small amount of intestinal epithelial cell necrosis, indicating the protective effect of SXD on the intestine of CDI mice (Fig. 1E and F).

3.2. Effect of SXD on the improvement of gut microbiota in CDI mice

Antibiotics can disrupt the normal barrier function of colon flora, providing a favorable environment for *C. difficile* colonization. Regulating the gut microbiota can alleviate CDI [18]. During treatment, we examined the effect of SXD on the gut microbiota. Fig. 2 and Fig. S4 illustrate the impact of SXD on the gut microbiota. Alpha diversity results indicated that CDI significantly decreased the abundance and diversity (Fig. 2 A-B, Fig. S4 A-B) of intestinal microflora in mice. After administration, SXD adjusted the richness and diversity of the intestinal flora of mice. Although SXD showed a reversed adjustment of the enteric bacteria, the timing of administration did not affect this result (Fig. 2 A-B, Fig. S4 A-B). The coverage indices of all groups of samples exceeded 99%, indicating that the sequencing results' coverage could reflect the actual community structure (Fig. S4 C). Based on the non-metric multidimensional scaling (NMDS, Fig. 2C) and principal coordinate analysis (PCoA, Fig. S4 D), beta Diversity analysis showed that CDI significantly altered the overall structure of intestinal flora, and the intestinal flora tended to return to the normal group after SXD treatment. The results of NMDS and PCoA showed that, although the distance between the SXD and MOD group was closer than the normal group, there were still evident differences between the SXD and MOD group. In summary, CDI disrupts the overall structure of the intestinal microbial group, and SXD can partially reverse this alteration.

Next, we aimed to identify differential taxa that were affected by CDI interference and (partly) restored by SXD. The Venn diagram revealed that 64 OTUs were present in all groups, while 416, 30, 56, 88, and 85 OTUs were uniquely present in the CON group,

D3_MOD group, D_3SXD group, D_7MOD group, and D_7SXD group, respectively. On the third day, the SXD group and the CON group had 32 OTUs in common, while the MOD group had only 2. On the seventh day, the number of overlaps in the SXD group increased to 43, and that in the MOD group increased to 32 OTUs (Fig. S5A). The relative abundance of phyla and genera in the five groups showed significant structural differences (Fig. 2D and E). The classified heat map also showed significant structural differences among the five groups (Figs. S4E–F). Previous studies have shown changes in Firmicutes and Bacteroidetes in patients with CDI [19]. At the phylum level, the 7-day relative abundance of Firmicutes was significantly increased in SXD, but the abundance of Bacteroidetes decreased (Fig. 2D and E). Using LEfSe (Fig. S5B–C), permutational MANOVA analysis, and *t*-test analysis, we determined the differences between taxa and preserved only those disturbed by CDI and revised by SXD. As a result, we identified 12 major taxa, including *Muribaculaceae* spp., *Faecalibaculum* spp., *Negativibacillus* spp., *Eubacterium* spp., *Helicobacter* spp., *Ruminococcus* spp., *Clostridia* spp., *Bifidobacterium* spp., *Lactobacillus* spp., *Peptococcaceae* spp., *Lachnoclostridium* spp., and *Lachnospiraceae* spp. In the 12 taxa, Eubacterium, Clostridia, Peptococcaceae, and Lachnospiraceae were found to decrease after CDI and increase after SXD treatment.

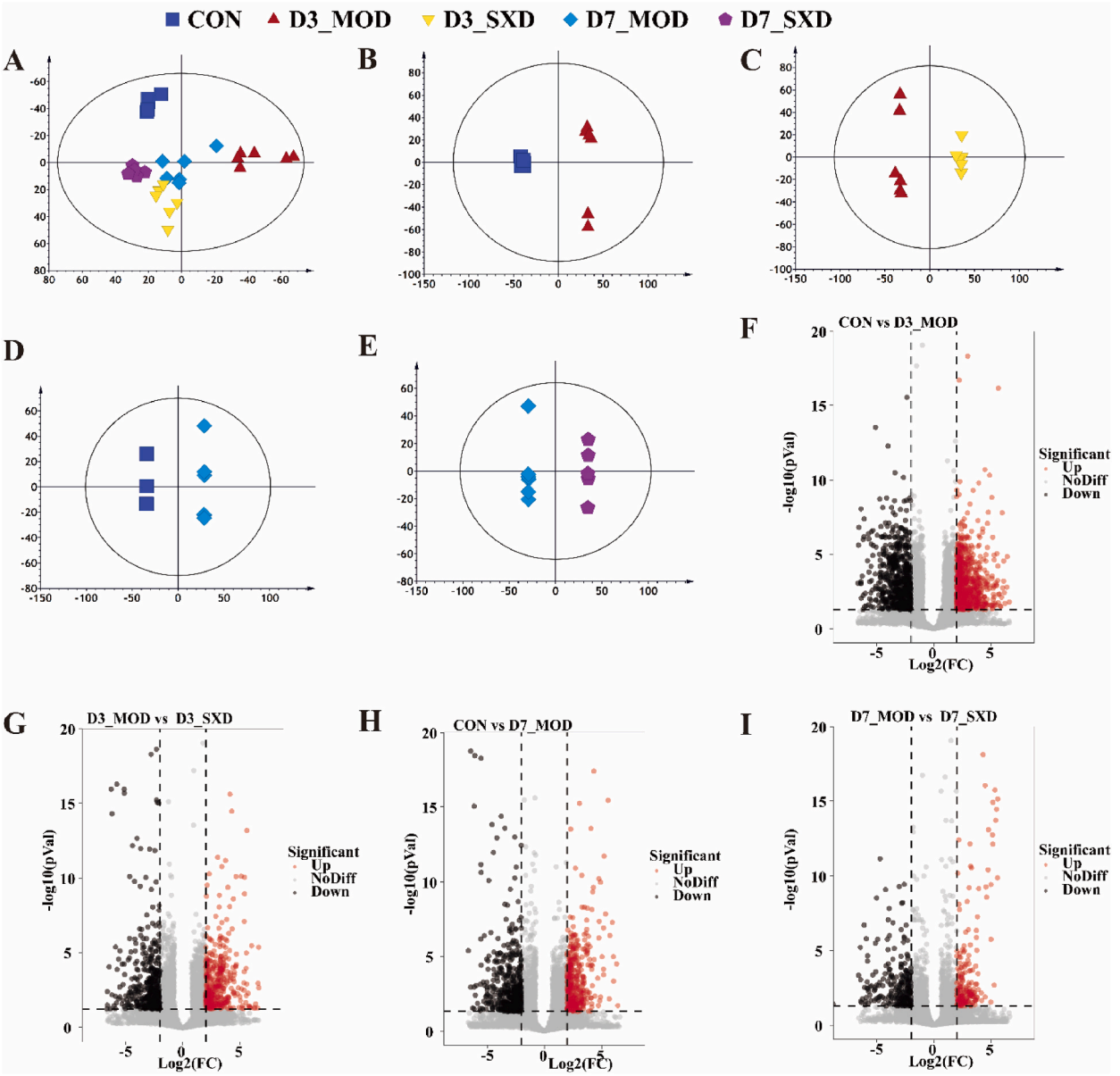

Fig. 3. Regulation of serum metabolism by SXD in ESI + mode. (A) PCA of variables in different groups. OPLS-DA score plots for pair-wise comparison between CON group and day3 MOD group (B), day3 MOD group and day3 SXD group (C), CON group and day7 MOD group (D), day7 MOD group and day7 SXD group (E). Volcano plot showing the differential variables between CON group and day3 MOD group (F), day3 MOD group and day3 SXD group (G), CON group and day7 MOD group (H), day7 MOD group and day7 SXD group (I). UP shows up-regulation, DW indicates down-regulation, and NoDiff shows no statistical difference.

3.3. The effects of SXD on serum metabolic

Studies have indicated that drug intake has a significant impact on serum metabolism [20]. The medication component in the blood can trigger a series of reactions that eventually lead to changes in the metabolic products of blood circulation. Therefore, we examined the serum metabolites of mice following SXD treatment. The effects of SXD on mouse serum metabolism are depicted in Figs. 3 and 4. The PCA score plot demonstrated that CDI can significantly alter the serum metabolomic profile in both positive and negative modes (Fig. 3A and Fig. S6A). Furthermore, SXD treatment restores the CDI-induced altered serum metabolic profile. The findings revealed that CDI can alter mice's serum metabolism, while SXD can correct this imbalance. Plots of OPLS-DA scores in positive mode show that the CDI groups can be clearly separated from the normal groups, and the SXD groups can be clearly separated from the MOD groups (Fig. 3B–E).Fig. S6 B-E also showed similar results using OPLS-DA scores in negative mode. OPLS-DA was found to be effective in screening differential metabolites. The variables whose content changed between the comparison groups were then plotted using volcano plots based on VIP value, P value, and fold change (Fig. 3 F–I and Fig. S6 F-I). The results identified 25 differential metabolites in serum (Table 2). Among these metabolic products, uridine, mitemcinal, glucoside, naphthoic acid, diphosphoglucuronic acid, L-ornithine, isobutylamide, D-glucoside, D-*glycero*-D-galacto-heptitol, dichloroacetate, 1,2-naphthoquinone, 3-indolebutyric acid, histidylglycine, dinoseb acetate, glycyl histidine, acridineacetic acid, cyclohexylammonium, succinylproline, hypotaurine, thymidine, carbamate, 2-thiouric acid, glycerol, L-threonine, and isopropyldichloromethyl ether were included (Fig. 4A–Y). SXD reversed the effects of CDI on ten metabolites that increased due to CDI treatment. Furthermore, CDI treatment reduced 15 metabolites, and SXD reversed the reduction caused by CDI in these 15 metabolites. We introduced the 25 differential metabolites into the metabolic analysis software to explore the possible anti-CDI mechanism of action of SXD. The results showed that there were eight metabolic pathways regulated by SXD (Fig. S7).

3.4. Identification of components in vivo

Base peak chromatograms (BPC) were obtained using UPLC-MS for both ion modes with the Thermo Xcalibur Qual Browser workstation. To identify the absorbed blood components, the BPI chromatograms of the in vitro samples, the model group, and the drug-administered samples acquired by UPLC-MS are shown in Fig. S8. The serum UPLC-MS data of MOD mice and SXD mice were analyzed using OPLS-DA. Compounds were selected for identification if their response value in the administration group was 1000 times greater than that in the control group, and the response value of SXD medicine was greater than 1000 (Fig. S9 A-B). The excimer ions of the compound were analyzed through pick peaking in the form of adduct ions, including [M+H], [M + H–2H2O], [M+Na], [M + FA-H], [M-H2O–H], [M − H], and [M+Cl]. Finally, by comparing sample retention times and accurate masses with those of the standards, and matching the single-flavored medicinal compounds in the TCM DataBase@Taiwan online database, 17 incorporated blood components were initially identified in the body. Among them, six compounds were detected in positive mode (Fig. S9 C), and 11 compounds were detected in negative mode (Fig. S9 D). These included Kaempferol-3-arabofuranoside, Catechin-5-O-glucoside (−), Suffruticoside A, Glycyrrhetinic acid, wogonin, Phebalosin, 6-gingerol, Isoliquiritin, methoxylutcolin, Ginsenoside-Rf, 6-Shogaol, Panaxadiol, 3-Hydroxyglabrol (II), Catechin-5-O-glucoside (+), Feruloyltyramine, Mycosinol, and berberrubine, as illustrated in

Table 2
List of differential serum metabolites.

NO.	Rt/min	*m/z*	Adducts	Fomula	Error/ppm	Compouds Name
1	2.69	243.0618	M − H $^-$	$C_9H_{12}N_2O_6$	1	Uridine
2	1.06	736.4624	M–H_2O–H $^-$	$C_{40}H_{69}NO_{12}$	2	Mitemcinal
3	7.34	361.1501	M–H_2O–H $^-$	$C_{16}H_{28}O_{10}$	1	Prenyl apiosyl-(1->6)-glucoside
4	8.01	187.039	M − H $^-$	$C_{11}H_8O_3$	1	1-Hydroxy-2-naphthoic acid
5	5.11	579.0326	M − H $^-$	$C_{15}H_{22}N_2O_{18}P_2$	1	Uridine 5′-diphosphoglucuronic acid
6	2.85	100.1123	M + H $^+$	$C_7H_{14}N_2O_3$	2	N2-Acetyl-L-ornithine
7	7.25	475.2064	M + K $^+$	$C_{20}H_{32}N_6O_5$	0	DN-isobutylamide
8	8.71	175.1074	M + H +	$C_8H_{10}N_4O_2$	2	D-Glucoside
9	8.81	195.0874	M + H–H_2O $^+$	$C_7H_{16}O_7$	2	D-Glycero-D-galacto-heptitol
10	9.34	195.0873	M + H $^+$	$C_2H_2Cl_2O_2$	1	Dichloroacetate
11	9.37	197.0002	M + K $^+$	$C_{10}H_6O_2$	1	1,2-Naphthoquinone
12	9.73	204.1008	M + H $^+$	$C_{12}H_{13}NO_2$	6	3-Indolebutyric acid
13	15.88	195.0874	M + H–H_2O $^+$	$C_8H_{12}N_4O_3$	4	Histidylglycine
14	8.96	226.0691	M + H $^+$	$C_{12}H_{14}N_2O_6$	4	Dinoseb acetate
15	8.76	195.0874	M + H–H_2O $^+$	$C_8H_{12}N_4O_3$	4	Glycyl-Histidine
16	8.75	275.0795	M + Na $^+$	$C_{15}H_{12}N_2O_2$	2	9-Oxo-10-acridineacetic acid
17	8.1	243.0968	M + H $^+$	$C_6H_{13}N$	2	cyclohexylammonium
18	6.3	283.0936	M + H $^+$	$C_9H_{13}NO_5$	1	Succinylcholine
19	5.15	147.9832	M + K $^+$	$C_2H_7NO_2S$	2	Hypotaurine
20	4.19	285.2203	M + H $^+$	$C_{10}H_{14}N_2O_5$	3	Thymidine
21	4.13	228.1201	M + Na $^+$	$C_9H_{19}NO_4$	2	*Tert*-Butyl (2- (2-hydroxyethoxy) ethyl) carbamate
22	2.76	206.9948	M + Na $^+$	$C_5H_4N_4O_2S$	1	2-Thiouric acid
23	0.98	115.0366	M + Na $^+$	$C_3H_8O_3$	0	Glycerol
24	0.84	192.9791	M + H–H_2O $^+$	$C_4H_5NO_7P$	2	4-phospho-hydroxy-L-threonine
25	0.6	164.9842	M + Na $^+$	$C_4H_8Cl_2O$	1	Isopropyldichloromethyl ether

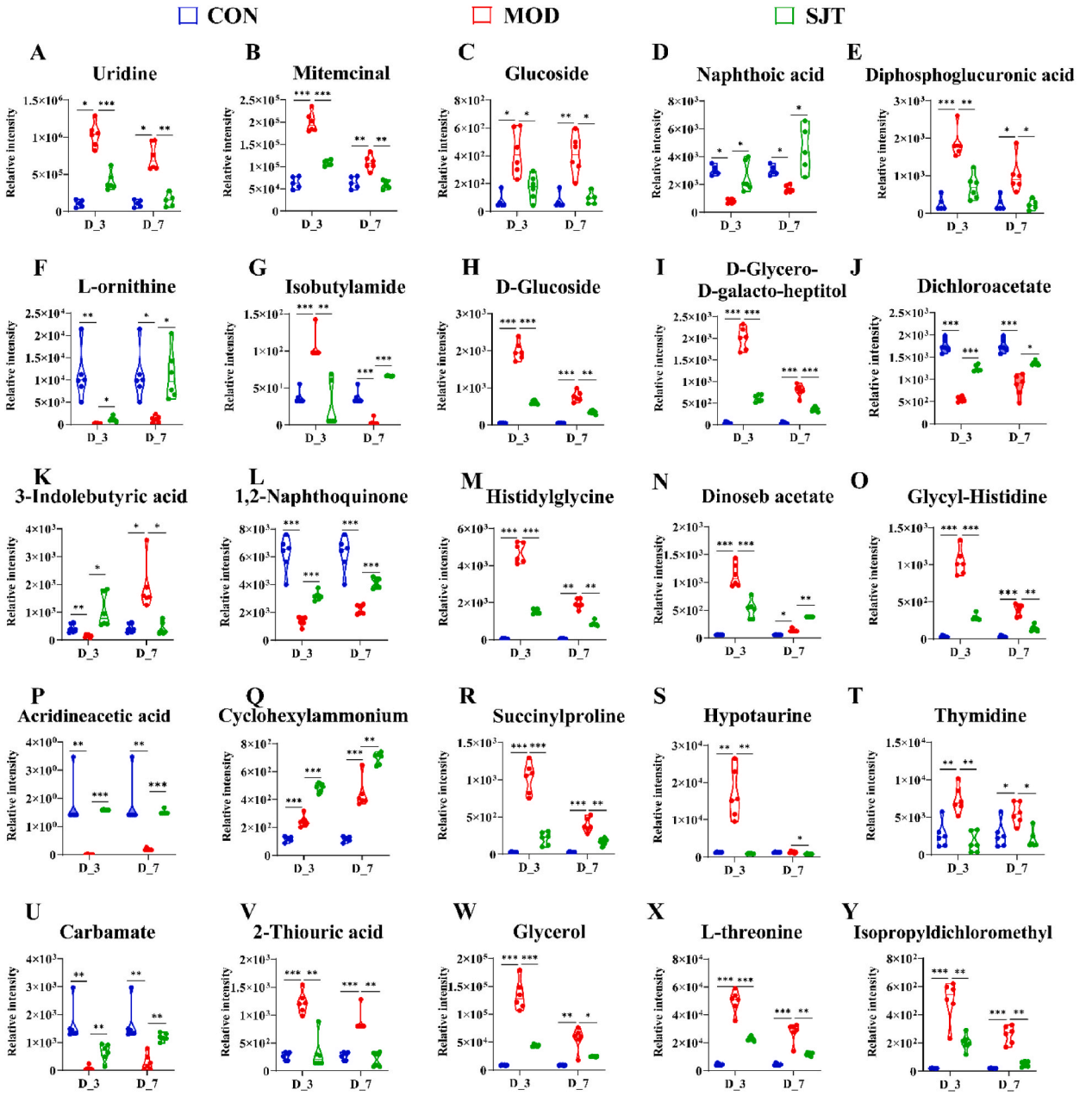

Fig. 4. The scatter plot shows the relative content and significant difference of serum metabolites in different groups (n = 5–6). *$P < 0.05$, **$P < 0.01$, ***$P < 0.001$.

Table 3 and Fig. S9.

3.5. *Comprehensive analysis of the treatment effect of SXD on CDI*

In this study, we have integrated data from four different latitudes, which include information about the gut microbiota classification, chemical composition of the drug in serum samples, metabolites present in serum samples, and pharmacodynamic data of SXD. Firstly, we calculated the inner layer correlations between the gut microbiota, serum drug composition, and serum metabolites (Fig. S11). Next, we calculated the correlations between the gut microbiota and serum drug composition, between the serum drug composition and serum metabolites, and between phenotype and all three factors (Fig. S11). To visualize the relationship between the gut microbiota, serum drug composition, serum metabolites, and pharmacodynamic data, we constructed an integrated network with three levels and four dimensions.

Table 3
Blood transitional components of SXD detected by UPLC-Q/TOF-MS in positive and negative ion modes.

NO.	Rt/min	*m/z*	Adducts	Fomula	Compouds Name	Source
1	8.22	277.1791	[M+H]+	$C_{17}H_{24}O_3$	6-Shogaol	A/B
2	8.5	425.3756	[M + H–2H_2O] +	$C_{30}H_{52}O_3$	Panaxadiol	C
3	5.09	373.1825	[M + H–2H_2O] +	$C_{25}H_{28}O_5$	3-Hydroxyglabrol (II)	D
4	7.31	435.1274	[M + H–H_2O] +	$C_{21}H_{24}O_{11}$	Catechin-5-O-glucoside (+)	E
5	7.84	336.1218	[M+Na] +	$C_{18}H_{19}NO_4$	Feruloyltyramine	E
6	10.12	215.0697	[M+H] +	$C_{13}H_{10}O_3$	Mycosinol	C
7	8.24	287.0947	[M + H–2H_2O] +	$C_{19}H_{16}NO_4$	berberrubine	F
8	6.48	463.088	[M + FA-H] -	$C_{20}H_{18}O_{10}$	Kaempferol-3-arabofuranoside	C
9	7.3	433.1136	[M–H_2O–H] -	$C_{21}H_{24}O_{11}$	Catechin-5-O-glucoside (-)	E
10	5.28	593.1507	[M–H_2O–H] -	$C_{27}H_{32}O_{16}$	Suffruticoside A	C
11	13.91	469.3319	[M − H] -	$C_{30}H_{46}O_4$	Glycyrrhetinic acid	D
12	10.54	283.0609	[M − H] -	$C_{16}H_{12}O_5$	wogonin	G
13	10.27	283.061	[M+Cl] -	$C_{15}H_{14}O_4$	Phebalosin	D
14	8.21	469.2074	[M − H] -	$C_{23}H_{34}O_{10}$	6-gingerol	A/B
15	8.12	431.0979	[M+Cl] -	$C_{21}H_{22}O_9$	Isoliquiritin	D
16	7.37	443.0981	[M–H_2O–H] -	$C_{22}H_{22}O_{11}$	methoxylutcolin	C
17	6.92	845.4884	[M + FA-H] -	$C_{42}H_{72}O_{14}$	Ginsenoside-Rf	C

A: *Zingiber officinale* Rosc. (fresh); B: *Zingiber officinale* Rosc. (dried); C: *Panax ginseng* C. A. Mey; D: *Glycyrrhiza uralensis* Fisch.; E: *Ziziphus jujuba* Mill.; F: *Coptis chinensis* Franch.; G: *Scutellaria baicalensis* Georgi.; (+) represents the positive ion mode, (−) represents the negative ion mode.

As a result, 12 taxa in the gut microbiota layer were integrated into the network, including *Muribaculaceae* spp., *Faecalibaculum* spp., *Clostridia* spp., *Lachnospiraceae* spp., and others. In the blood components layer, 17 blood transitional components were integrated into the network, including Panaxadiol, Ginsenoside-Rf, methoxylutcolin, and others. A total of 25 metabolites from the serum metabolism layer were integrated into the network, including Uridine, Mitemcinal, Thymidine, Hypotaurine, and others. Three drug efficacy data were integrated into the network. In the comprehensive analysis of the network, each edge denotes a significant correlation between two indicators ($|r|>0.5$, $P < 0.05$). After analyzing the combined network, it was observed that the top ten most correlated indicators exclusively consisted of blood components of SXD, specifically Panaxadiol, Methoxylutcolin, Ginsenoside-Rf,

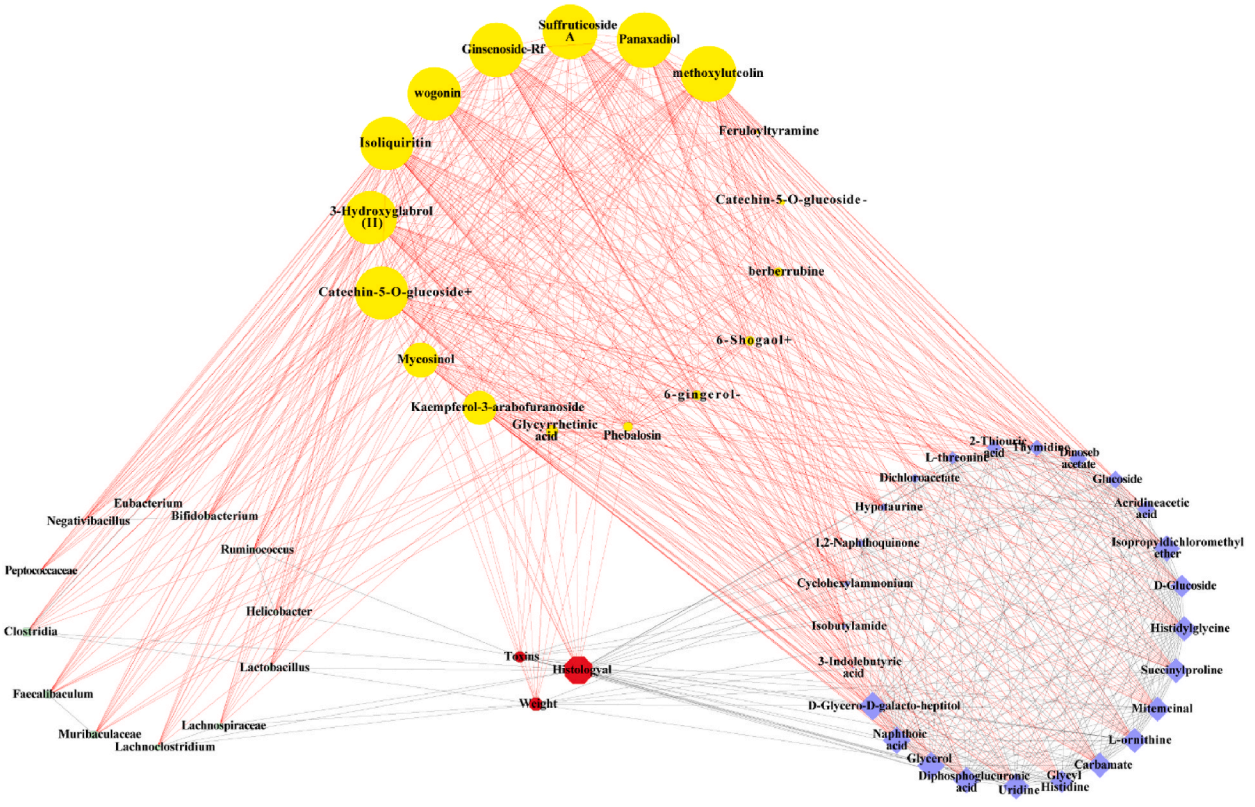

Fig. 5. The integrated therapeutic mechanism of SXD in treating CDI. The edges are the correlations with Spearman's correlation coefficient <–0.6 (or >0.6) and $P < 0.05$.

Suffruticoside A, Catechin-5-O-glucoside+, 3-Hydroxyglabrol (II), Isoliquiritin, Wogonin, Mycosinol, and Kaempferol-3-arabofuranoside. This observation indicates that the aforementioned components play an indispensable role in the efficacious treatment of CDI by SXD. Furthermore, lymph nodes in the gut microbiota layer and towards the component layer were less relevant than lymph nodes in the other two layers (Fig. 5). The integrated network provides a comprehensive view of SXD's therapeutic mechanism in the treatment of CDI.

4. Discussion

With the increasing use of antibiotics, the incidence of CDI is on the rise, and its causes are complex and diverse. Further study is needed to understand the pathogenesis [7,21]. TCM has the characteristics of abundant resources, low cost, and few side effects, and it plays an important role in the Chinese medical system. Some studies have shown that herbal medicines have good efficacy against CDI [22]. The combination of TCM and antibiotics can prevent recurrent infections caused by antibiotic treatment [23]. Ancient medical texts describe SXD as a Chinese prescription for intestinal inflammation and diarrhea. Scientific evidence for SXD is accumulating, including clinical efficacy evaluations and characterization of complex components [24,25]. However, Chinese medicine prescriptions contain many complex ingredients and only substances that are absorbed in the serum after oral administration are considered pharmacodynamic. Therefore, to explore the pharmacodynamic material basis and mechanism of SXD in treating CDI to the greatest extent, we carried out serum component identification, untargeted metabolomics analysis, and fecal 16S DNA sequencing analysis after SXD was administered to normal mice. In addition, we also constructed a multiscale network to visualize the mechanisms of SXD.

The intestinal microbiota is known to play a crucial role in preventing CDI by hindering the colonization of *C. difficile* [18], while the use of antibiotics promotes the growth of *C. difficile* and leads to the development of CDI [26]. In this study, CDI mice that had decreased levels of Firmicutes and increased levels of Bacteroidetes were found to have their phylum-level flora restored after treatment with SXD. Furthermore, at the genus level, *Muribaculaceae* spp., *Ruminococcus* spp., *Bifidobacterium* spp., and *Lachnospiraceae* spp. were detected after SXD administration, indicating that SXD could help improve the diversity and richness of the intestinal microbiota in mice and restore its balance.

Primary bile acids are synthesized in living organisms and are involved in all functions of the intestinal tract, making them important metabolites of the lower gastrointestinal tract. Bile acid metabolism is thought to be closely related to CDI [7,27]. Cholic acids and chenodeoxyglycocholic acid, which are primary bile acids, are synthesized in the liver, combined with taurine or glycine, and then secreted into the intestinal tract through bile [28,29]. Previous studies have shown that taurine and hypotaurine can protect against oxidative stress-induced pathologies, including damage to the gastrointestinal tract, and that the downregulation of taurine may indicate inflammatory reactions [30,31]. The CDI group in this study had higher hypotaurine levels than the control group, indicating disordered taurine and hypotaurine metabolism. SXD was found to affect hemoglobin synthesis, heme decomposition, biliverdin reduction, and bilirubin metabolism. The disorder in taurine and hypotaurine metabolism was clearly improved in the SXD group, suggesting that SXD may treat CDI by modulating hypotaurine levels.

Subsequent analysis revealed that the MOD group had disruptions in Ascorbate and Aldarate metabolism, Glycerolipid metabolism, Pentose and Glucuronate interconversions, Pyrimidine metabolism, and other metabolic pathways. These pathways were significantly regulated after SXD administration. All of these pathways are closely related to amino acid and energy metabolism, and the regulation of Ascorbate and Aldarate metabolism can improve the intestinal microbiota and inhibit intestinal inflammation [32,33]. Glycerolipid metabolism and Pentose and Glucuronate interconversions are both strongly associated with the restoration of intestinal function and the overall metabolic environment [34,35], while Pyrimidine metabolism is closely related to the digestive system, and improving disorders of Pyrimidine metabolism can reduce intestinal inflammation and modulate the disrupted intestine [36,37]. These findings suggest that SXD may ameliorate and treat CDI by regulating these metabolic pathways.

According to the theory and method of serum pharmacochemistry, drugs enter the blood, get metabolized and distributed, and then produce specific biological effects through specific mechanisms. Blood components are the ultimate "effective components." We have characterised 17 substances of SXD *in vivo* that are highly correlated with drug efficacy. These 17 compounds were extracted from 7 components of SXD. According to the Integrated network analysis, the highly correlated blood components included the 6-Shogaol and 6-gingerol from *Zingiber officinale* Rosc. (fresh) and *Zingiber officinale* Rosc. (dried); Panaxadiol, Mycosinol, Kaempferol-3-arabofuranoside, Suffruticoside A, methoxylutcolin and Ginsenoside-Rf from *Panax ginseng* C. A. Mey; 3-Hydroxyglabrol (II), Glycyrrhetinic acid, Phebalosin and Isoliquiritin from *Glycyrrhiza uralensis* Fisch.; Catechin-5-O-glucoside, Feruloyltyraminefrom from *Ziziphus jujuba* Mill.; berberrubine from *Coptis chinensis* Franch.; Wogonin from *Scutellaria baicalensis* Georgi (Table 3). The results of previously conducted studies have shown that the main herb in the prescription, *Zingiber officinale* Rosc., has good efficacy in digestive disorders.

According to the theory and method of serum pharmacochemistry, drugs enter the bloodstream, undergo metabolism and distribution, and then produce specific biological effects through specific mechanisms. The ultimate "effective components" are the blood components. We have characterized 17 substances of SXD *in vivo* that are highly correlated with drug efficacy. These 17 compounds were extracted from 7 components of SXD.

According to integrated network analysis, the highly correlated blood components included 6-Shogaol and 6-gingerol from fresh and dried *Zingiber officinale* Rosc.; Panaxadiol, Mycosinol, Kaempferol-3-arabofuranoside, Suffruticoside A, Methoxylutcolin, and Ginsenoside-Rf from Panax ginseng C. A. Mey; 3-Hydroxyglabrol (II), Glycyrrhetinic acid, Phebalosin, and Isoliquiritin from Glycyrrhiza uralensis Fisch.; Catechin-5-O-glucoside, Feruloyltyramine from Ziziphus jujuba Mill.; Berberrubine from Coptis chinensis Franch.; and Wogonin from Scutellaria baicalensis Georgi (Table 3).

Previous studies have shown that the main herb in the prescription, Zingiber officinale Rosc., has good efficacy in treating digestive

disorders [38], Extracts from this herb, 6-Shogaol and 6-gingerol, have been shown to prevent and treat liver damage and intestinal barrier damage [39], inhibit intestinal inflammation [40], and exhibit intestinal spasmolytic activity [41]. Ginsenoside-Rf from Panax ginseng C. A. Mey has been found to treat dextran sodium sulfate-induced ulcerative colitis in mice by suppressing IL-6 and DNF-α [42]. Glycyrrhetinic acid, a pentacyclic triterpenoid and one of the main active ingredients of *Glycyrrhiza uralensis* Fisch., and its derivatives have been found to possess various pharmacological activities such as anti-inflammatory, anti-viral, and anti-tumor effects [43]. Berberine has been found to inhibit the TLR4 pathway, which reduces the intestinal damage caused by LPS and thus ameliorates ileal and systemic inflammation [44]. The results of the current study indicate that oral administration of berberine had therapeutic effects in animals with experimental chronic ulcerative colitis. These effects included reductions in intestinal fibrosis and remodeling, protection of intestinal barrier function, and inflammatory infiltrations [45]. These substances may be active components of SXD when treating CDI *in vivo*.

To gain a comprehensive understanding of SXD's active ingredients on CDI, we constructed an associative network comprising information on gut microbiota, serum metabolomics, blood components, and phenotypes. The network was constructed based on Spearman's correlation coefficient. Although the network is associative rather than causal, it still provides valuable information on understanding SXD's active ingredients. All 17 blood components were included in the integrated network and were significantly correlated with gut microflora, serum metabolites, and phenotype. The most crucial components include Panaxadiol, Methoxylutcolin, Ginsenoside-Rf, Suffruticoside A, Catechin-5-O-glucoside, 3-Hydroxyglabrol (II), Isoliquiritin, Wogonin, Mycosinol, and Kaempferol-3-arabofuranoside. Most of these components are categorized as tonic and warming herbs, such as *Panax ginseng* C. A. Mey, *Glycyrrhiza uralensis* Fisch., and *Ziziphus jujuba* Mill., which is consistent with the Traditional Chinese Medicine (TCM) theory of "strengthening vital qi to eliminate pathogenic factors."

5. Conclusion

Our study shows that SXD can alleviate CDI, and its therapeutic effects are linked to its ability to modulate gut microbiota composition and serum metabolism. We explored the efficacy and active ingredients of SXD for treating CDI by integrating serum pharmacochemistry and serum metabolomics. Our results indicate that the 17 components of SXD are significantly correlated with differential metabolites and flora in mice and may exert therapeutic effects by modulating relevant pathways. These findings shed light on the mechanisms and active ingredients of SXD for treating CDI.

Author contribution statement

Zhi-jie Ma: Conceived and designed the experiments; Contributed reagents, materials, analysis tools or data.

Xuemei Qin: Contributed reagents, materials, analysis tools or data.

Yutao Cui, Cong-en Zhang: Conceived and designed the experiments; Performed the experiments; Analyzed and interpreted the data; Wrote the paper.

Xueqiang Zhang, Xiaohong Yu, Yuqin Ma: Performed the experiments; Analyzed and interpreted the data.

Data availability statement

Data will be made available on request.

Declaration of competing interest

The authors declare that they have no known financial or interpersonal conflicts that might have looked to have influenced the research presented in this study.

Acknowledgments

This work was supported by the financial support of the National Natural Science Foundation of China (no. 82004032), the Beijing Hospitals Authority Youth Programme (code: QML20210107), and the Young Elite Scientists Sponsorship Program by CACM (no. QNRC2-C13) are gratefully acknowledged.

Appendix A. Supplementary data

Supplementary data to this article can be found online at https://doi.org/10.1016/j.heliyon.2023.e15602.

References

[1] A. Krishna, T. Chopra, Prevention of infection due to Clostridium (clostridioides) difficile, Infect. Dis. Clin. 35 (4) (2021) 995–1011, https://doi.org/10.1016/j.idc.2021.07.009.

[2] C. Aguayo, R. Flores, S. Levesque, P. Araya, S. Ulloa, J. Lagos, J.C. Hormazabal, J. Tognarelli, D. Ibanez, P. Pidal, O. Duery, B. Olivares, J. Fernandez, Rapid spread of Clostridium difficile NAP1/027/ST1 in Chile confirms the emergence of the epidemic strain in Latin America, Epidemiol. Infect. 143 (14) (2015) 3069–3073, https://doi.org/10.1017/S0950268815000023.

[3] N.O. Markham, S.C. Bloch, J.A. Shupe, E.N. Laubacher, A.K. Thomas, H.K. Kroh, K.O. Childress, F.C. Peritore-Galve, M.K. Washington, R.J. Coffey, D.B. Lacy, Murine intrarectal instillation of purified recombinant clostridioides difficile toxins enables mechanistic studies of pathogenesis, Infect. Immun. 89 (4) (2021), https://doi.org/10.1128/IAI.00543-20.

[4] M.J. Alfa, A. Kabani, D. Lyerly, S. Moncrief, L.M. Neville, A. Al-Barrak, G.K. Harding, B. Dyck, K. Olekson, J.M. Embil, Characterization of a toxin A-negative, toxin B-positive strain of Clostridium difficile responsible for a nosocomial outbreak of Clostridium difficile-associated diarrhea, J. Clin. Microbiol. 38 (7) (2000) 2706–2714, https://doi.org/10.1128/JCM.38.7.2706-2714.2000.

[5] T. Akerlund, B. Svenungsson, A. Lagergren, L.G. Burman, Correlation of disease severity with fecal toxin levels in patients with Clostridium difficile-associated diarrhea and distribution of PCR ribotypes and toxin yields in vitro of corresponding isolates, J. Clin. Microbiol. 44 (2) (2006) 353–358, https://doi.org/10.1128/JCM.44.2.353-358.2006.

[6] D. Lyras, J.R. O'Connor, P.M. Howarth, S.P. Sambol, G.P. Carter, T. Phumoonna, R. Poon, V. Adams, G. Vedantam, S. Johnson, D.N. Gerding, J.I. Rood, Toxin B is essential for virulence of Clostridium difficile, Nature 458 (7242) (2009) 1176–1179, https://doi.org/10.1038/nature07822.

[7] M.C. Abt, P.T. McKenney, E.G. Pamer, Clostridium difficile colitis: pathogenesis and host defence, Nat. Rev. Microbiol. 14 (10) (2016) 609–620, https://doi.org/10.1038/nrmicro.2016.108.

[8] A. Durovic, S. Tschudin-Sutter, Cutting edges in Clostridioides difficile infections, Swiss Med. Wkly. 151 (2021), w30033, https://doi.org/10.4414/smw.2021.w30033.

[9] H.Y. Guan, X.M. Wang, S.P. Wang, Y. He, J.J. Yue, S.G. Liao, Y.D. Huang, Y. Shi, Comparative intestinal bacteria-associated pharmacokinetics of 16 components of Shengjiang Xiexin decoction between normal rats and rats with irinotecan hydrochloride (CPT-11)-induced gastrointestinal toxicity in vitro using salting-out sample preparation and LC-MS/MS, RSC Adv. 7 (69) (2017) 43621–43635, https://doi.org/10.1039/c7ra03521g.

[10] C. Deng, B. Deng, L. Jia, H. Tan, P. Zhang, S. Liu, Y. Zhang, A. Song, L. Pan, Preventive effects of a Chinese herbal formula, shengjiang Xiexin decoction, on irinotecan-induced delayed-onset diarrhea in rats, Evid. Bas. Comp. Alter. Med. (2017), 7350251, https://doi.org/10.1155/2017/7350251, 2017.

[11] C. Deng, Y. Lou, Y. Gao, B. Deng, F. Su, L. Jia, Efficacy and safety of Shengjiang Xiexin decoction in prophylaxis of chemotherapy-related diarrhea in small cell lung cancer patients: study protocol for a multicenter randomized controlled trial, Trials 21 (1) (2020) 370, https://doi.org/10.1186/s13063-020-04275-5.

[12] J. Wang, L.Q. Jia, H.Y. Tan, L. Pan, L.L. Yu, B. Deng, [Effect of shengjiang Xiexin decoction on the repair of damaged rat intestinal mucosa after irinotecan chemotherapy], Zhongguo Zhong Xi Yi Jie He Za Zhi 35 (10) (2015) 1236–1243.

[13] S. Li, N.L. Sullivan, N. Rouphael, T. Yu, S. Banton, M.S. Maddur, M. McCausland, C. Chiu, J. Canniff, S. Dubey, K. Liu, V. Tran, T. Hagan, S. Duraisingham, A. Wieland, A.K. Mehta, J.A. Whitaker, S. Subramaniam, D.P. Jones, A. Sette, K. Vora, A. Weinberg, M.J. Mulligan, H.I. Nakaya, M. Levin, R. Ahmed, B. Pulendran, Metabolic phenotypes of response to vaccination in humans, Cell 169 (5) (2017) 862–877 e817, https://doi.org/10.1016/j.cell.2017.04.026.

[14] X.D. Hao, X.N. Chen, Y.Y. Zhang, P. Chen, C. Wei, W.Y. Shi, H. Gao, Multi-level consistent changes of the ECM pathway identified in a typical keratoconus twin's family by multi-omics analysis, Orphanet J. Rare Dis. 15 (1) (2020) 227, https://doi.org/10.1186/s13023-020-01512-7.

[15] R. Knight, A. Vrbanac, B.C. Taylor, A. Aksenov, C. Callewaert, J. Debelius, A. Gonzalez, T. Kosciolek, L.I. McCall, D. McDonald, A.V. Melnik, J.T. Morton, J. Navas, R.A. Quinn, J.G. Sanders, A.D. Swafford, L.R. Thompson, A. Tripathi, Z.Z. Xu, J.R. Zaneveld, Q. Zhu, J.G. Caporaso, P.C. Dorrestein, Best practices for analysing microbiomes, Nat. Rev. Microbiol. 16 (7) (2018) 410–422, https://doi.org/10.1038/s41579-018-0029-9.

[16] Y. Han, H. Sun, A. Zhang, G. Yan, X.J. Wang, Chinmedomics, a new strategy for evaluating the therapeutic efficacy of herbal medicines, Pharmacol. Ther. 216 (2020), 107680, https://doi.org/10.1016/j.pharmthera.2020.107680.

[17] W. Yang, Y. Zhang, W. Wu, L. Huang, D. Guo, C. Liu, Approaches to establish Q-markers for the quality standards of traditional Chinese medicines, Acta Pharm. Sin. B 7 (4) (2017) 439–446, https://doi.org/10.1016/j.apsb.2017.04.012.

[18] R.A. Britton, V.B. Young, Role of the intestinal microbiota in resistance to colonization by Clostridium difficile, Gastroenterology 146 (6) (2014) 1547–1553, https://doi.org/10.1053/j.gastro.2014.01.059.

[19] T.J. Louie, M.A. Miller, K.M. Mullane, K. Weiss, A. Lentnek, Y. Golan, S. Gorbach, P. Sears, Y.K. Shue, O.P.T.C.S. Group, Fidaxomicin versus vancomycin for Clostridium difficile infection, N. Engl. J. Med. 364 (5) (2011) 422–431, https://doi.org/10.1056/NEJMoa0910812.

[20] J. Liu, L. Lahousse, M.G. Nivard, M. Bot, L. Chen, J.B. van Klinken, C.S. Thesing, M. Beekman, E.B. van den Akker, R.C. Slieker, E. Waterham, C.J.H. van der Kallen, I. de Boer, R. Li-Gao, D. Vojinovic, N. Amin, D. Radjabzadeh, R. Kraaij, L.J.M. Alferink, S.D. Murad, A.G. Uitterlinden, G. Willemsen, R. Pool, Y. Milaneschi, D. van Heemst, H.E.D. Suchiman, F. Rutters, P.J.M. Elders, J.W.J. Beulens, A. van der Heijden, M.M.J. van Greevenbroek, I.C.W. Arts, G.L. J. Onderwater, A. van den Maagdenberg, D.O. Mook-Kanamori, T. Hankemeier, G.M. Terwindt, C.D.A. Stehouwer, J.M. Geleijnse, L.M. Hart, P.E. Slagboom, K. W. van Dijk, A. Zhernakova, J. Fu, B. Penninx, D.I. Boomsma, A. Demirkan, B.H.C. Stricker, C.M. van Duijn, Integration of epidemiologic, pharmacologic, genetic and gut microbiome data in a drug-metabolite atlas, Nat. Med. 26 (1) (2020) 110–117, https://doi.org/10.1038/s41591-019-0722-x.

[21] D. VanInsberghe, J.A. Elsherbini, B. Varian, T. Poutahidis, S. Erdman, M.F. Polz, Diarrhoeal events can trigger long-term Clostridium difficile colonization with recurrent blooms, Nat. Microb. 5 (4) (2020) 642–650, https://doi.org/10.1038/s41564-020-0668-2.

[22] G. Ya-Nan, W. Jun, Z. Hao-Jun, J. Hong-Bing, L. Ping, L. Xin-Zhu, Traditional Chinese medicine QPYF as preventive treatment for Clostridium difficile associated diarrhea in a mouse model, Evid. Bas. Comp. Alter. Med. (2016), 3759819, https://doi.org/10.1155/2016/3759819, 2016.

[23] Z. Lv, G. Peng, W. Liu, H. Xu, J. Su, Berberine blocks the relapse of Clostridium difficile infection in C57BL/6 mice after standard vancomycin treatment, Antimicrob. Agents Chemother. 59 (7) (2015) 3726–3735, https://doi.org/10.1128/AAC.04794-14.

[24] H.Y. Guan, P.F. Li, X.M. Wang, J.J. Yue, Y. He, X.M. Luo, M.F. Su, S.G. Liao, Y. Shi, Shengjiang Xiexin decoction alters pharmacokinetics of irinotecan by regulating metabolic enzymes and transporters: a multi-target therapy for alleviating the gastrointestinal toxicity, Front. Pharmacol. 8 (2017) 769, https://doi.org/10.3389/fphar.2017.00769.

[25] G. Peng, H. Guan, X. Wang, Y. Shi, Simultaneous determination of 14 active constituents of Shengjiang Xiexin decoction using ultrafast liquid chromatography coupled with electrospray ionization tandem mass spectrometry, Acta Pharm. Sin. B 7 (2) (2017) 193–201, https://doi.org/10.1016/j.apsb.2016.11.006.

[26] P. Feuerstadt, Clostridium difficile infection, Clin. Transl. Gastroenterol. 6 (2015) e92, https://doi.org/10.1038/ctg.2015.13.

[27] J.D. Kang, C.J. Myers, S.C. Harris, G. Kakiyama, I.K. Lee, B.S. Yun, K. Matsuzaki, M. Furukawa, H.K. Min, J.S. Bajaj, H. Zhou, P.B. Hylemon, Bile acid 7alpha-dehydroxylating gut bacteria secrete antibiotics that inhibit Clostridium difficile: role of secondary bile acids, Cell Chem. Biol. 26 (1) (2019) 27–34 e24, https://doi.org/10.1016/j.chembiol.2018.10.003.

[28] D.W. Russell, The enzymes, regulation, and genetics of bile acid synthesis, Annu. Rev. Biochem. 72 (2003) 137–174, https://doi.org/10.1146/annurev.biochem.72.121801.161712.

[29] A.F. Hofmann, L.R. Hagey, Bile acids: chemistry, pathochemistry, biology, pathobiology, and therapeutics, Cell. Mol. Life Sci. 65 (16) (2008) 2461–2483, https://doi.org/10.1007/s00018-008-7568-6.

[30] J. Bai, Y. Zhu, Y. Dong, Modulation of gut microbiota and gut-generated metabolites by bitter melon results in improvement in the metabolic status in high fat diet-induced obese rats, J. Funct.Foods 41 (2018) 127–134, https://doi.org/10.1016/j.jff.2017.12.050.

[31] J. Zhou, N. Yao, S. Wang, D. An, K. Cao, J. Wei, N. Li, D. Zhao, L. Wang, X. Chen, Y. Lu, Fructus Gardeniae-induced gastrointestinal injury was associated with the inflammatory response mediated by the disturbance of vitamin B6, phenylalanine, arachidonic acid, taurine and hypotaurine metabolism, J. Ethnopharmacol. 235 (2019) 47–55, https://doi.org/10.1016/j.jep.2019.01.041.

[32] S.T. Fang, T. Qin, T. Yu, G.X. Zhang, Improvement of the gut microbiota in vivo by a short-chain fatty acids-producing strain lactococcus garvieae CF11, Processes 10 (3) (2022). ARTN 60410.3390/pr10030604.

[33] Q. Qi, Y.N. Liu, X.M. Jin, L.S. Zhang, C. Wang, C.H. Bao, H.R. Liu, H.G. Wu, X.M. Wang, Moxibustion treatment modulates the gut microbiota and immune function in a dextran sulphate sodium-induced colitis rat model, World J. Gastroenterol. 24 (28) (2018) 3130–3144, https://doi.org/10.3748/wjg.v24.i28.3130.

[34] M.L. Jin, J.J. Wang, H. Zhang, H.B. Zhou, K. Zhao, Simulated weightlessness perturbs the intestinal metabolomic profile of rats, Front. Physiol. 10 (2019). ARTN 127910.3389/fphys.2019.01279.
[35] X. Xiong, J. Zhou, H.N. Liu, Y.L. Tang, B. Tan, Y.L. Yin, Dietary lysozyme supplementation contributes to enhanced intestinal functions and gut microflora of piglets, Food Funct. 10 (3) (2019) 1696–1706, https://doi.org/10.1039/c8fo02335b.
[36] Y.L. Liu, C.Y. Xie, Z.Y. Zhai, Z.Y. Deng, H.O.R. De Jonge, X. Wu, Z. Ruan, Uridine attenuates obesity, ameliorates hepatic lipid accumulation and modifies the gut microbiota composition in mice fed with a high-fat diet, Food Funct. 12 (4) (2021) 1829–1840, https://doi.org/10.1039/d0fo02533j.
[37] B.L. Li, P.L. Du, Y. Du, D.Y. Zhao, Y.R. Cai, Q. Yang, Z.J. Guo, Luteolin alleviates inflammation and modulates gut microbiota in ulcerative colitis rats, Life Sci. 269 (2021). ARTN 11900810.1016/j.lfs.2020.119008.
[38] Y. Kim, D.M. Kim, J.Y. Kim, Ginger extract suppresses inflammatory response and maintains barrier function in human colonic epithelial caco-2 cells exposed to inflammatory mediators, J. Food Sci. 82 (5) (2017) 1264–1270, https://doi.org/10.1111/1750-3841.13695.
[39] X.X. Guo, Y.D. Zhang, T.C. Wang, X.L. Wang, Y.Y. Xu, Y. Wang, J. Qiu, Ginger and 6-gingerol prevent lipopolysaccharide-induced intestinal barrier damage and liver injury in mice, J. Sci. Food Agric. 102 (3) (2022) 1066–1075, https://doi.org/10.1002/jsfa.11442.
[40] B.O. Ajayi, I.A. Adedara, E.O. Farombi, 6-Gingerol abates benzo[a]pyrene-induced colonic injury via suppression of oxido-inflammatory stress responses in BALB/c mice, Chem. Biol. Interact. 307 (2019) 1–7, https://doi.org/10.1016/j.cbi.2019.04.026.
[41] M.N. Ghayur, A.H. Gilani, Species differences in the prokinetic effects of ginger, Int. J. Food Sci. Nutr. 57 (1–2) (2006) 65–73, https://doi.org/10.1080/09637480600656074.
[42] S. Ahn, S.Y. Simu, D.C. Yang, M. Jang, B.H. Um, Effects of Ginsenoside Rf on dextran sodium sulfate-induced colitis in mice, Food Agric. Immunol. 32 (1) (2021) 360–372, https://doi.org/10.1080/09540105.2021.1950128.
[43] S.Y. Wu, S.C. Cui, L. Wang, Y.T. Zhang, X.X. Yan, H.L. Lu, G.Z. Xing, J. Ren, L.K. Gong, 18beta-Glycyrrhetinic acid protects against alpha-naphthylisothiocyanate-induced cholestasis through activation of the Sirt1/FXR signaling pathway, Acta Pharmacol. Sin. 39 (12) (2018) 1865–1873, https://doi.org/10.1038/s41401-018-0110-y.
[44] Q. Zhang, X.L. Piao, X.S. Piao, T. Lu, D. Wang, S.W. Kim, Preventive effect of Coptis chinensis and berberine on intestinal injury in rats challenged with lipopolysaccharides, Food Chem. Toxicol. 49 (1) (2011) 61–69, https://doi.org/10.1016/j.fct.2010.09.032.
[45] H. Li, C. Feng, C. Fan, Y. Yang, X. Yang, H. Lu, Q. Lu, F. Zhu, C. Xiang, Z. Zhang, P. He, J. Zuo, W. Tang, Intervention of oncostatin M-driven mucosal inflammation by berberine exerts therapeutic property in chronic ulcerative colitis, Cell Death Dis. 11 (4) (2020) 271, https://doi.org/10.1038/s41419-020-2470-8.